Solid-State NMR Structure Determination of Melittin in a Lipid Environment

Y.-H. Lam,* S. R. Wassall,† C. J. Morton,* R. Smith,‡ and F. Separovic*

*School of Chemistry, University of Melbourne, Melbourne VIC 3010, Australia; †Department of Physics, Indiana University/Purdue University, Indianapolis, Indiana 46202 USA; and ‡Department of Biochemistry, University of Queensland, Brisbane QLD 4072, Australia

ABSTRACT Solid-state ^{13}C NMR spectroscopy was used to investigate the three-dimensional structure of melittin as lyophilized powder and in ditetradecylphosphatidylcholine (DTPC) membranes. The distance between specifically labeled carbons in analogs [1-^{13}C]Gly3-[2-^{13}C]Ala4, [1-^{13}C]Gly3-[2-^{13}C]Leu6, [1-^{13}C]Leu13-[2-^{13}C]Ala15, [2-^{13}C]Leu13-[1-^{13}C]Ala15, and [1-^{13}C]Leu13-[2-^{13}C]Leu16 was measured by rotational resonance. As expected, the internuclear distances measured in [1-^{13}C]Gly3-[2-^{13}C]Ala4 and [1-^{13}C]Gly3-[2-^{13}C]Leu6 were consistent with α-helical structure in the N-terminus irrespective of environment. The internuclear distances measured in [1-^{13}C]Leu13-[2-^{13}C]Ala15, [2-^{13}C]Leu13-[1-^{13}C]Ala15, and [1-^{13}C]Leu13-[2-^{13}C]Leu16 revealed, via molecular modeling, some dependence upon environment for conformation in the region of the bend in helical structure induced by Pro14. A slightly larger interhelical angle between the N- and C-terminal helices was indicated for peptide in dry or hydrated gel state DTPC (139°–145°) than in lyophilized powder (121°–139°) or crystals (129°). The angle, however, is not as great as deduced for melittin in aligned bilayers of DTPC in the liquid-crystalline state (~160°) (R. Smith, F. Separovic, T. J. Milne, A. Whittaker, F. M. Bennett, B. A. Cornell, and A. Makriyannis, 1994, *J. Mol. Biol.* 241:456–466). The study illustrates the utility of rotational resonance in determining local structure within peptide-lipid complexes.

INTRODUCTION

Lipid-protein interactions are important in a large number of fundamental processes occurring at the surface of the cell, such as the anchoring and stabilization of membrane-bound proteins (Bernëche et al., 1998). Many biophysical techniques, including x-ray crystallography (Deisenhofer and Michel, 1989), electron microscopy (Henderson et al., 1990), NMR spectroscopy (Cross and Opella, 1994), and computer simulation (Bernëche et al., 1998), provide insight into the structure of membrane proteins in different environments. Precise three-dimensional structural characterization of membrane proteins remains difficult, however, because of the inapplicability of the two standard high-resolution methods, x-ray crystallography and solution-state NMR spectroscopy. The lack of long-range order in membranes restricts the use of x-ray diffraction, whereas the size of realistic protein-lipid complexes is too large for high-resolution solution NMR techniques. Consequently, the conformation of less than a handful of membrane-bound proteins has been solved. Often membrane peptides are used to gain insight into membrane protein structure. Melittin is one such peptide that has been studied using many different biophysical techniques (Terwilliger and Eisenberg, 1982; Inagaki et al., 1989; Bazzo et al., 1988; Okada et al., 1994). In nanomolar amounts, melittin can form ion channels (Tosteson and Tosteson, 1981), whereas at higher concentrations it causes membrane disruption that leads to cell lysis (Bazzo et al., 1988; Okada et al., 1994; Tosteson and Tosteson, 1981) by a mechanism that remains unclear. Detailed structural studies of membrane peptides such as melittin may serve as a model for understanding other membrane-binding polypeptides (Segrest et al., 1990) and ion translocation mechanisms in more complex systems.

Melittin is an amphipathic peptide of 26 amino acids with primary sequence GIGAVLKVLTTGLPALISWIKRKRQQ-$CONH_2$. The peptide is the major toxin in honey bee (*Apis mellifera*) venom and, as mentioned above, is responsible for lysis of cell membranes (Sessa et al., 1969). The proline at position 14 and the polar residues 23–26 at the C-terminus are important for the lytic action of melittin (Otoda et al., 1992; Rivett et al., 1996; Warwicker and Waston, 1982). The conformation of melittin in membrane-like environments and in the aqueous phase has been studied using several techniques. Melittin in crystalline form (Terwilliger and Eisenberg, 1982), in dodecylphosphocholine (DPC) micelles (Inagaki et al., 1989), in methanol (Bazzo et al., 1988), and in vesicles (Okada et al., 1994) adopts a helical conformation (Talbot et al., 1979; Dawson et al., 1978; Knoppel et al., 1979; Bello et al., 1982), consisting of two α-helical segments separated by a kink at proline-14. At low concentrations in aqueous solution, melittin is monomeric and has no persistent three-dimensional structure (Terwilliger and Eisenberg, 1982; Dempsey, 1990). At higher concentrations, particularly at high ionic strength, it forms a tetramer with a predominantly helical content (Terwilliger and Eisenberg, 1982). The x-ray structure obtained from crystals grown from aqueous solution has two α-helical segments that make an angle[2] of ~120° at proline-14 (Ter-

Received for publication 17 May 2001 and in final form 19 July 2001.

C. J. Morton's current address: Department of Biochemistry and Molecular Biology, Monash University, Clayton, VIC 3800 Australia.

Address reprint requests to Dr. Frances Separovic, University of Melbourne, School of Chemistry, Melbourne VIC 3010, Australia. Tel. 61-3-8344-6464; Fax: 61-3-9347-5180; E-mail: fs@unimelb.edu.au.

0006-3495/01/11/2752/10 $2.00

williger and Eisenberg, 1982). In methanol (160° ± 20°) (Bazzo et al., 1988) and DPC micelles (135° ± 15°) (Inagaki et al., 1989), this angle is found to be closer to the average of 154° ± 5° between helical segments noted for proline-containing helices in crystallized proteins (Barlow and Thornton, 1988). A substantially different value of 86° ± 34° is observed in phospholipid vesicles (Okada et al., 1994). (Note that the interhelical angles stated here are directly quoted from the literature. Care should be exercised in comparing these values because they are sensitive to the number of residues employed to define each helix.)

Melittin adopts different locations, orientations, and association states within membranes under different conditions (Dempsey, 1990). In bilayer systems, melittin may occupy two locations; it either remains on the bilayer surface or takes up a transmembrane orientation. In different lipids (Dawson et al., 1978; Drake and Hider, 1979; Vogel, 1981, 1987; Vogel and Jähnig, 1986) and at two hydration levels (6% w/w and 30% w/w), infrared techniques have shown that the orientation of the melittin is with the α-helical segments oriented roughly perpendicular to the plane of the membrane (Dempsey, 1990). Neutron diffraction studies (Dempsey, 1990) of melittin in oriented, fluid-phase lipid show that melittin-bound deuterons are located at the bilayer surface. A location parallel to the bilayer plane at the depth of the glycerol groups was also concluded for the helical axis in aligned dioleoylphosphatidylcholine at low peptide concentration and hydration on the basis of x-ray diffraction data (Hristova et al., 2001). Recently, molecular dynamics simulations have examined the interaction of melittin with a fully hydrated dimyristoylphosphatidylcholine (DMPC) bilayer (Bernëche et al., 1998; Bachar and Becker, 2000; Lin and Baumgaertner, 2000). Bachar and Becker (2000) suggest that melittin adopts a 25° tilt relative to the membrane normal with the N-terminus embedded in the membrane perpendicular to the surface in a transbilayer orientation. It should be acknowledged that in the simulation, an initial transbilayer orientation was assumed.

In our earlier NMR study (Smith et al., 1994), the orientation of melittin in lipid was determined using an aligned membrane system with ^{13}C-labeled melittin analogs incorporated into bilayers in a 15:1 lipid:melittin ratio, with 50% w/v hydration. The peptide was found to be well aligned in the bilayers and reorienting about the bilayer normal. The same experiments showed there was no apparent difference in the orientation or motion of residues in the regions that form separate helices in the water-soluble form of the peptide. This suggested that in membranes the angle between the helices is greater than the 120° observed in the crystal form and closer to the 160° observed in methanol (Bazzo et al., 1988).

The study of melittin in model membranes may be useful for the development of techniques for the determination of membrane protein structures. Solid-state NMR methods such as rotational resonance (RR) that have been developed over the last decade have tremendous potential to provide details of local structure within membrane-incorporated peptides (Peersen and Smith, 1993; Peersen et al., 1995). This technique requires isotopic labeling to allow measurement of the internuclear distance between pairs of labeled sites and entails reintroducing the dipolar coupling that is removed by magic angle spinning (MAS). Inter-nuclear distances for peptides within a lipid bilayer can be determined with an accuracy of ± 0.2 Å. In this paper we report RR measurements of melittin lyophilized from different solvents and dispersed with phospholipid in lyophilized powder and following hydration, with particular focus on the angle of the bend around the proline at position 14.

MATERIALS AND METHODS

Materials

^{13}C-labeled amino acids, [1-^{13}C]Gly, [1-^{13}C]Ala, [2-^{13}C]Ala, [1-^{13}C]Leu, and [2-^{13}C]Leu (99% enrichment) were purchased from Cambridge Isotope Laboratory (Woburn, MA). Rink-modified TentaGel resin, 9-fluorenylmethoxycarbonyl (FMOC)-amino acids, *O*-benzotriazole-*N*,*N*,*N*′,*N*′,-tetramethyl-uronium-hexafluorophosphate (HBTU), *N*-hydroxybenzotriazole (HOBt), benzotriazole-1-yl-oxy-tris-pyrrolidino-phosphonium-hexafluorophosphate (PyBOP), piperidine, diisopropylethylamine (DIPEA), and trifluoroacetic acid (TFA) were obtained from Auspep (Melbourne, Australia). Triethylsilane was obtained from Aldrich (St. Louis, MO).

Native melittin (70% purity) was purchased from Sigma (St. Louis, MO) and purified by high-performance liquid chromatography (HPLC) on a C18 column (Zorbax 300SB, 4.6 × 250 mm, 300-Å pore size), using a gradient of acetronitrile in 0.1% TFA. 1,2-Ditetradecylphosphatidylcholine (DTPC) was bought from Avanti Polar Lipids (Alabaster, AL).

Peptide synthesis

Synthesis of FMOC-protected amino acids

FMOC amino acids were synthesized using two different methods to give pure products with high yield. FMOC-[1-^{13}C]alanine was produced using the method of Fields et al. (1989) whereas FMOC-[2-^{13}C]leucine and FMOC-[1-^{13}C]glycine were made using the method of Carpino and Han (1972) with, respectively, yields of 60% and 84% for the two methods. All three products were characterized by ^{1}H and ^{13}C solution NMR and HPLC.

Synthesis of melittin

The following site-specific labeled analogs of melittin were studied: [1-^{13}C]Gly3-[2-^{13}C]Ala4 melittin, [1-^{13}C]Gly3-[2-^{13}C]Leu6 melittin, [1-^{13}C]Leu13-[2-^{13}C]Ala15 melittin, [2-^{13}C]Leu13-[1-^{13}C]Ala15 melittin, and [1-^{13}C]Leu13-[2-^{13}C]Leu16 melittin. The first four analogs were kindly donated by F. G. Prendergast, Mayo Foundation (Rochester, MN). Duplicate samples of these doubly labeled melittins and the fifth analog were synthesized by FMOC-chemistry using Rink-modified TentaGel resin (0.5 g, 0.1 mmol scale synthesis) and manual solid-phase techniques (Stewart and Stewart, 1984). The resin was first swollen with dichloromethane for 30 min and then with dry *N*,*N*-dimethylformamide (DMF) for an additional 45 min. The first FMOC-protected amino acid (0.5 mmol) was attached to the resin via an amide bond. This was activated by coupling reagents: HOBt (34 mg, 0.5 mmol), HBTU (95 mg, 0.5 mmol), and DIPEA (200 μl) in 2 ml of dry DMF, which were added to the resin and mixed for 2 h. Double couplings on the first amino acid and other difficult residues

(valine, leucine, proline, and the labeled amino acids) were carried out to ensure complete reaction. The removal of the FMOC group was achieved using 25% piperidine in DMF (5 ml for 20 min). Completion of each coupling and the deprotection step were confirmed by the Kaiser test (Kaiser et al., 1970). Once the whole sequence was synthesized, the resin was washed three times with dichloromethane, then with methanol, and finally with ether and dried overnight. The peptide was cleaved from the resin in 95% TFA with 2.5% H_2O and 2.5% triethylsilane, and rinsed three times with 2 ml of TFA. The combined filtrates were evaporated down to 1 ml under N_2 gas, and cold ether was added to precipitate the peptide. The precipitate was centrifuged and the solvent decanted. After drying to remove the residual solvent, the peptide was purified by HPLC and characterized by mass spectroscopy and ^1H and ^{13}C solution NMR.

Sample preparation

Melittin analogs were studied in three forms: lyophilized powder, dry lipid dispersions, and hydrated lipid bilayers. In each case, a corresponding natural abundance sample was prepared for the purpose of background spectral subtraction. The samples, which typically contained 2–4 mg of peptide, were prepared as follows. For lyophilized powders, peptides were dissolved in methanol and freeze-dried using a liquid nitrogen cold-trap. One sample was freeze-dried from water for comparison. For dry lipid dispersions, melittin was co-dissolved in methanol with DTPC in 1:15 molar ratio. The samples were then lyophilized overnight. For hydrated lipid bilayers, dry DTPC/melittin samples were mixed with MilliQ water (50% w/w) by centrifuging back and forth through a narrow constriction at a temperature above the gel-liquid crystalline transition temperature, T_C = 25°C (Smith et al., 1994). Samples were transferred to rotors for MAS experiments.

Solid-state NMR spectroscopy

Solid-state NMR spectroscopy was carried out on a Varian Inova 300 (Varian, Palo Alto, CA) equipped with a Doty MAS probe (Doty Scientific, Columbia, SC). The operating frequencies were 75.45 MHz for ^{13}C and 121.44 MHz for ^{31}P, while ^1H decoupling and cross-polarization were applied at 300.04 MHz.

Rotational resonance (RR) is a MAS experiment that detects the rotation-driven transfer of Zeeman magnetization between like spins (typically ^{13}C pairs) that occurs when the frequency of sample spinning, ν_r, matches the condition $\Delta\nu = n\nu_r$, where $\Delta\nu$ is the isotropic chemical shift difference in Hz between the resonances and n is a small integer (Peersen and Smith, 1993). After initial signal enhancement by cross-polarization, the signal is restored to the z direction by a flip-back pulse. One of the two labeled-site resonances is then selectively inverted, and the exchange of longitudinal magnetization between nuclei as a function of mixing time, τ_m, is monitored with the aid of an observation pulse. From the change in intensity of the two labeled sites the dipolar coupling can be extracted using computer analysis (based on a program developed by M. H. Levitt, University of Stockholm, and generously provided by A. Watts, University of Oxford) which searches zero quantum T_2 (T_{2ZQ}) and dipolar coupling parameters for the best fit of the experimental data. The dipolar coupling, D_{IS}, is related to the interatomic spacing, r_{IS}, according to $r_{IS} = (\gamma_I\gamma_S h/4\pi^2 D_{IS})^{1/3}$ (Peersen et al., 1995; Levitt et al., 1992), where $\gamma_{I,S}$ are the gyromagnetic ratio for spins I and S, and h is Planck's constant. T_{2ZQ} is the time constant of zero quantum magnetization transfer from the energy state $\alpha\beta$ to $\beta\alpha$ (where α, β are the spin states of the two dipolar coupled spins I, S) and is similar to T_2 or the spin-spin relaxation time constant. The accuracy of the RR experiment is ~0.5 Å with precision ~0.1 Å (Peersen et al., 1995; Levitt et al., 1992) where 0.5 Å applies at the upper distance limit of r_{IS} = 6.5 Å, whereas at shorter distances the uncertainty is less.

The parameters used in RR experiments for all samples were as follows: spinning speed controlled to within ±0.1% for n = 1 (8807 or 9085 Hz) and n = 2 (4418 or 4623 Hz); recycle delay, 1s; ^1H and ^{13}C $\pi/2$ pulse width, 3.6 μs; number of scans, 4,800–12,000; contact time, 3.5 ms; selective π pulse of the order 220 μs; and sweep width, 30 kHz. Chemical shifts were referenced to tetramethylsilane. Experiments were repeated to determine the level of precision for the distance determination, and the estimated error was the range from different experimental observations.

RR data were obtained at ambient temperature (~25°C) and also at low temperatures (−30°C and −70°C). The temperature within the MAS sample was calibrated using lead nitrate as a chemical shift thermometer (Bielecki and Burum, 1995) with a shift of 0.455 ppm/°C and controlled within ±0.1°C. At low temperature, sample cooling was performed using boil-off N_2 gas on the MAS bearing line cooled by an exchange dewar filled with liquid nitrogen.

For hydrated lipid samples, broadline ^1H-decoupled ^{31}P NMR spectra were recorded at 30°C and −70°C to confirm, from the chemical shift anisotropy (CSA), that the lipid was in the bilayer phase (Seelig, 1978; Dufourc et al., 1992). A ^{31}P $\pi/2$ pulse of 3.6 μs, recycle delay of 3s, sweep width of 62 kHz, ^1H decoupling of 60 kHz, and 4,096–22,000 scans were used. Chemical shift was referenced to H_3PO_4 (85%).

Molecular modeling

Dynamics algorithm for NMR applications (DYANA) (Güntert et al., 1997) was used to model the structure for melittin incorporating the RR data. The atomic coordinates for melittin as crystal (Terwilliger and Eisenberg, 1982) and in DPC micelles (Inagaki et al., 1989) were used to determine local structural constraints for structure calculations. The strategy used in the structure calculations was to start with random structures and use constraints derived from the x-ray (Terwilliger and Eisenberg, 1982) or NMR (Inagaki et al., 1989) structures. The local conformation of the N- and C-terminal helices was constrained by the torsion angles to the values derived from the published structures ± 1° for residues 1–12 and 17–26. For residues 13–16, less restrictive constraints of the torsion angles were applied with a range of ±20° given to the published values, and the distances determined by RR were included as additional constraints. RR distances were given a relative weighting of 10 in the DYANA constraints to bias the final structures toward these values. Little effect on the final structure was observed if the torsion angles for residues 1–12 and 17–26 were either held essentially constant or allowed to vary by ±20° during the structure calculation. The larger range of angles was searched for residues 13–16, for which the internuclear distances measured by RR exhibited sensitivity to environment. Fifty structures were determined by simulated annealing in DYANA, and the best 10 were inspected and analyzed using the software package MOLMOL (Koradi et al., 1996). Inter-nuclear distances and the inter-helix angles for the x-ray and DPC structures were also measured in MOLMOL. An alternative modeling package, SYBYL 6.5 (Tripos, St. Louis, MO), was used to generate melittin structures using the same constraints to confirm the consistency of the technique.

RESULTS AND DISCUSSION

Melittin was synthesized with amino acids ^{13}C labeled at the α carbon [2-C] and carbonyl carbon [1-C] to measure internuclear distances using RR. Five doubly labeled melittin analogs (Fig. 1) were studied. The analogs [1-^{13}C]Leu13-[2-^{13}C]Ala15, [2-^{13}C]Leu13-[1-^{13}C]Ala15, and [1-^{13}C]Leu13-[2-^{13}C]Leu16 were used to probe peptide conformation in the region of the bend in helical structure induced by Pro14, which constitutes the major focus of this study. The analogs [1-^{13}C]Gly3-[2-^{13}C]Ala4 and [1-^{13}C]Gly3-[2-^{13}C]Leu6 labeled near the N-terminus were used to calibrate the RR experiment and confirm the maintenance of helical structure in

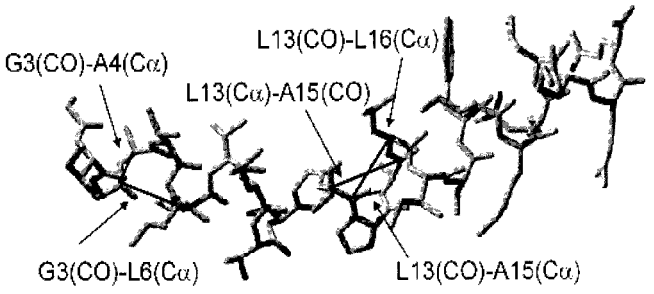

FIGURE 1 X-ray crystal structure of melittin (Terwilliger and Eisenberg, 1982) showing the five interatomic distances measured by RR between the doubly ^{13}C-labeled sites of the five synthetic labeled melittin analogs.

the peptide. For example, the [1-C]Gly3-[2-C]Ala4 distance is fixed at 2.4 Å, and [1-C]Gly3-[2-C]Leu6 is 4.4 Å in a helical structure but 9.6 Å in a fully extended structure (measured for model peptides using MOLMOL).

RR experiments were carried out by selectively inverting one of the ^{13}C-labeled resonances using a soft π pulse and observing the subsequent exchange of magnetization between labeled resonances while performing MAS at a spin rate satisfying the condition ($\Delta\nu = n\nu_r$) (Peersen and Smith, 1993). A range of mixing times τ_m was employed to follow the magnetization transfer. Fig. 2 *A* illustrates the process for [1-^{13}C]Leu13-[2-^{13}C]Ala 15 as a lyophilized powder in DTPC. As τ_m is increased, greater magnetization transfer between the two labeled carbons occurs, and the signal intensity of each resonance decreases. Analysis requires that spectra from samples containing native (natural abundance) melittin under identical conditions be subtracted to remove the background signal. Differences in peak intensity $\langle I_z - S_z \rangle$, normalized to 1 at zero mixing time, were then plotted against τ_m to generate a magnetization exchange curve (Peersen and Smith, 1993; Peersen et al., 1995). The plot shown for [1-^{13}C]Leu13-[2-^{13}C]Ala 15 with dry DTPC in Fig. 2 *B* is typical.

From the decay in magnetization transfer and the magnitude and orientation of the chemical shift tensor (Peersen and Smith, 1993; Peersen et al., 1995), the dipolar coupling, and hence the intermolecular distance between the two ^{13}C-labeled nuclei, can be derived. RR experiments were performed at spinning speeds satisfying both $n = 1$ and $n = 2$ to improve confidence in the results. On the one hand, the $n = 1$ condition is preferable because analysis is essentially insensitive to the relative orientation of the ^{13}C chemical shift tensors (Peersen and Smith, 1993), which is not precisely known. On the other hand, the stability of spinning speed upon which the RR method critically depends was better at $n = 2$. Thus, $n = 1$ was used to determine the accuracy and $n = 2$ the precision of the measurements. The data points in Fig. 2 *B* were obtained from experiment ($n = 1$), and the line drawn through the points represents a nonlinear least-squares fit to the magnetization exchange curve optimizing zero-quantum relaxation T_{2ZQ} and the dipolar coupling D_{IS} (Levitt et al., 1992). Fig. 2 *C* is a contour plot illustrating the square of the deviation (χ^2) between experiment and calculation as a function of D_{IS} and T_{2ZQ}, in a brute-force search through an appropriate range of both parameters to locate a global minimum error value. The range of dipolar couplings was chosen based on an extended range of anticipated interatomic distances between the two ^{13}C-labeled nuclei. An estimate of the lower limit for T_{2ZQ} was estimated according to the relationship $1/T_{2ZQ} = 1/T_2^I + 1/T_2^S$, or $T_{2ZQ} = 1/(\pi(\upsilon^I + \upsilon^S))$, where $\upsilon^{I,S}$ is the linewidth of ^{13}C resonances measured away from the RR condition, i.e., when $\Delta\nu \neq n\nu_r$, and the superscripts designate individual signal (Thompson et al., 1992). An upper limit to T_{2ZQ} was selected to ensure that a well-defined minimum in χ^2 was reached. Initially, the upper limit of T_{2ZQ} was chosen to be about twice the lower limit derived from linewidth, and then a narrower range in T_{2ZQ} was searched around the χ^2 minimum. Each value of T_{2ZQ} and dipolar coupling was taken to be equally likely.

Inter-nuclear distances in several site-specific labeled analogs of melittin, either as lyophilized powders or in dry and hydrated lipid, were determined by RR. In Table 1, they are compared with the corresponding distances obtained using x-ray diffraction of crystalline peptide (Terwilliger and Eisenberg, 1982) and solution NMR of peptide in DPC micelles (Inagaki et al., 1989). The precision of our experiments was typically ±0.1 Å in the dry powder and ±0.2 Å in the lipid bilayer, in agreement with Peersen and Smith (1993). Accuracy is dependent on the stability of the sample spinning speed, knowledge of the chemical shift tensor, and T_{2ZQ} (zero-quantum relaxation). Unlike $n = 1$, for RR conditions satisfying $n > 1$, calculation of the homonuclear distance is dependent on the relative orientation of chemical shift tensors. The ^{13}C chemical shift tensor values of Separovic et al. (1990) were used, and RR distances measured in melittin were confirmed by spinning at $n = 1$ and $n = 2$ as mentioned above. From our results, the accuracy and the precision of the RR measurements appeared to be similar, with an uncertainty better than ±0.2 Å.

Inspection of Table 1 reveals similar interatomic distances near the N-terminus were obtained by RR and from published x-ray diffraction and solution NMR structures (Terwilliger and Eisenberg, 1982; Inagaki et al., 1989), suggesting that the α-helical structure in this region was preserved. Reassuringly, for [1-C]Gly3-[2-C]Ala4 the distance (2.4–2.5 Å) in each case was identical within experimental uncertainty, which indicates that the accuracy of our RR measurements was close to 0.1 Å for this distance. For [1-^{13}C]Gly3-[2-^{13}C]Leu6 there was good agreement between the dry powder measurement by RR (4.6 Å) and the x-ray crystal structure (4.4 Å), whereas with DTPC (5.0 Å) and in DPC micelles (4.8 Å) the distances are slightly longer but mutually consistent (giving an average distance of 4.5 Å for melittin and 4.9 Å for melittin in lipid by the different

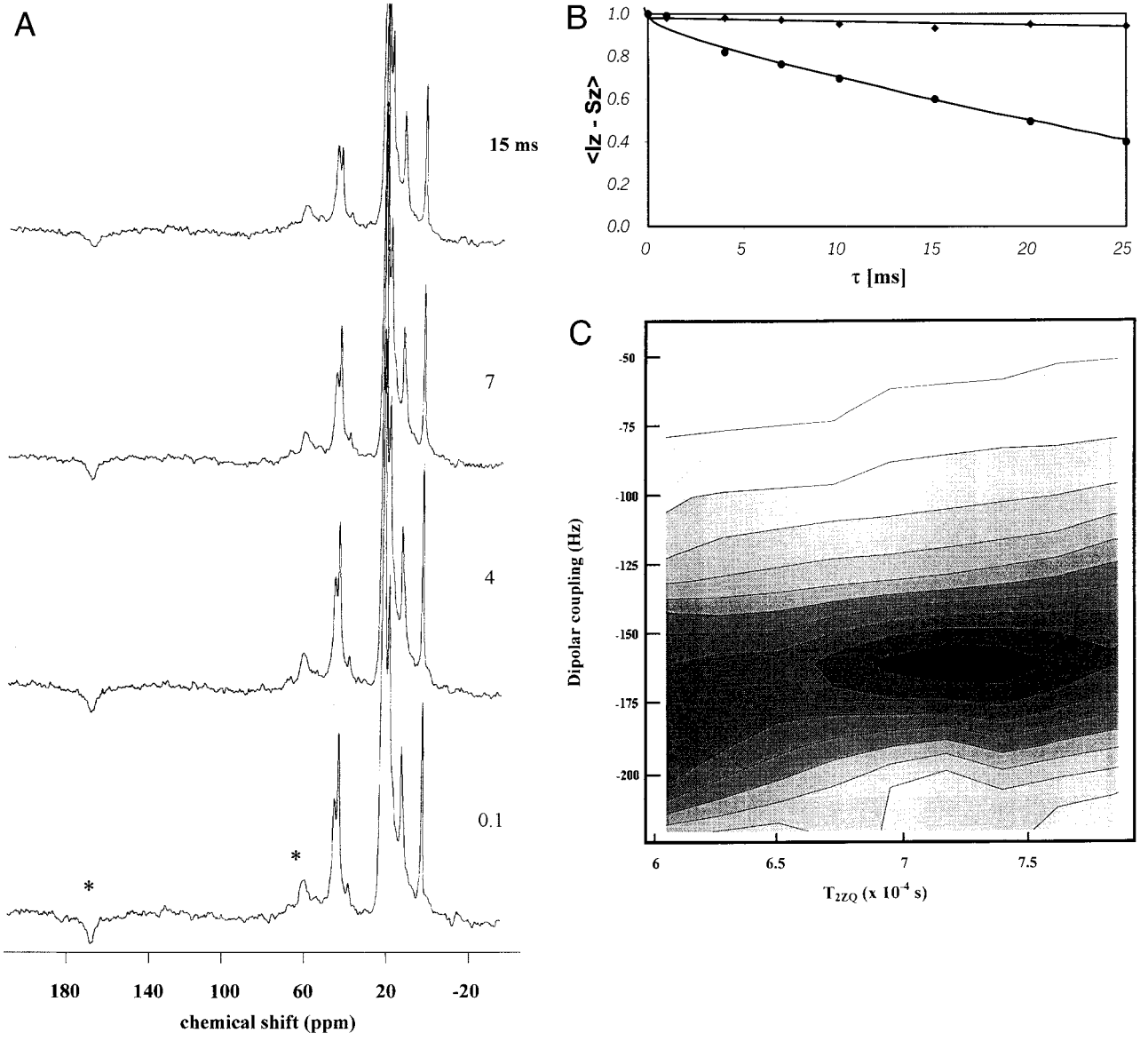

FIGURE 2 (*A*) RR spectra of [1-^{13}C]Leu13-[2-^{13}C]Ala15 melittin in dry DTPC showing the results obtained from a selection of mixing times: 0.1, 4, 7, and 15 ms. The spectra were acquired at ambient probe temperature with $n = 1$ and conditions as stated in Materials and Methods with 12,000 scans. The labeled carbonyl of melittin (4 mg) was selectively inverted. The increase in mixing time results in a decrease in signal for both the labeled Cα (60 ppm) and carbonyl (177 ppm) of melittin marked with an asterisk. The resonances around 10–50 ppm are the CH and CH_2 groups of the ether-linked lipid, DTPC. (*B*) The magnetization exchange curve determined from the RR spectra for [1-^{13}C]Leu13-[2-^{13}C]Ala15 melittin in dry DTPC (●) and, for comparison, an off-rotational resonance ($n = 1$) decay curve, 2 kHz below the RR condition (◆). The symbols on the graph are the data points obtained from experiment, and the fitted curve was obtained by nonlinear least-squares fitting of T_{2ZQ} and the dipolar coupling. (*C*) Contour plot of the square of the deviation (χ^2) between experiment and calculated values used to obtain the best fit of T_{2ZQ} and dipolar coupling to the RR data. The contours increment over a range in χ^2 of 4.4×10^{-4} to 8.0×10^{-4}.

techniques). These differences in interatomic distance may indicate a dependence of the peptide structure upon environment that was also evident in the region of the proline.

It is instructive to first compare the interatomic distances measured by RR on melittin as lyophilized powder with the values derived from the x-ray crystal structure. The situation with [1-^{13}C]Leu13-[2-^{13}C]Ala15 is particularly interesting. The interatomic distance by RR was 4.0 Å (±0.1 Å) when lyophilized from methanol and 4.7 Å when lyophilized from water, indicating a structural dependence based on environment. In the x-ray crystal structure the equivalent distance is 4.5 Å. Thus, it appears that the structure of melittin lyophilized from methanol resembles more closely that in DPC micelles, where the distance is 4.1 Å. When lyophilized from water, however, the RR distance was closer to that of the published x-ray structure than the solution NMR struc-

TABLE 1 Inter-nuclear distances in melittin

Melittin	RR of dry peptide (Å)	RR in DTPC (Å)	X-ray (Å)	Solution NMR (Å)
[1-^{1}C]Cly3-[2-^{13}C]Ala4	2.4	2.5	2.4	2.4
[1-^{13}C]Gly3-[2-^{13}C]Leu6	4.6	5.0	4.4	4.8
[1-^{13}C]Gly3-[2^{13}C]Ala15	4.0 4.7*	3.8	4.5	4.1
[2-^{13}C]Leu13-[1-^{13}C]Ala15	5.2	5.0	5.5	5.1
[1[^{13}C]Leu13-[2-^{13}C]Leu16	4.3	4.8	4.5	4.3

RR of peptide lyophilized from methanol and in DTPC (dry or hydrated gel phase), x-ray of crystalline peptide (Terwilliger and Eisenberg, 1982), and solution-state NMR of peptide in DPC micelles (Inagaki *et al.*, 1989).
*Samply lyophilized from water.

ture. This is most likely because the crystals used in x-ray experiments were grown from aqueous solution. When lyophilized from methanol, the more hydrophobic solvent may result in a structure more like that found in DPC micelles used in solution NMR. Less conformational sensitivity to environment is implied for [2-^{13}C]Leu13-[1-^{13}C]Ala15 and [1-^{13}C]Leu13-[2-^{13}C]Leu16 melittins. The RR distances in powders lyophilized from methanol were 5.2 Å and 4.3 Å, respectively, for the two analogs whereas the corresponding x-ray crystal values are 5.5 Å and 4.5 Å. The differences of 0.2–0.3 Å are within experimental error.

The conformation of melittin incorporated into DTPC was studied using a 15:1 lipid:peptide ratio to allow comparison with earlier work in aligned DTPC multilayers (Smith et al., 1994). DTPC, an ether-linked phosphatidylcholine (PC), was chosen to allow the observation of the peptide carbonyl resonance without spectral overlap from the lipid carbonyl resonances of ester-linked lipids (Smith et al., 1994). Distance measurements in lyophilized samples of melittin in DTPC in the absence and presence of 50% w/v water were undertaken. To confirm that the samples were in lamellar phase, broadline ^{1}H-decoupled ^{31}P NMR spectra were obtained. Examples of ^{31}P spectra of lyophilized and hydrated samples of [1-^{13}C]Leu13-[2-^{13}C]Ala15 melittin in DTPC are shown in Fig. 3, *A* and *B*, respectively. The spectrum in Fig. 3 *A* is a broadened axially symmetric powder pattern characteristic of lipids in a gel-like lamellar phase, indicating that the sample is not entirely free of water (Seelig, 1978; Dufourc et al., 1992). It should be noted that in the gel phase, the ether-linked PC may adopt an interdigitated bilayer phase (Laggner et al., 1991; Hing et al., 1991; Kim et al., 1987a,b). In Fig. 3 *B*, the spectrum with 50% w/v water at 30°C shows a narrowed spectrum with CSA on the order of −45 ppm, establishing that the lipid was in the fluid bilayer phase.

In dry DTPC the RR experiments were carried at probe ambient temperature (~25°C) whereas in hydrated lipid the samples were run at low temperature (~−30°C and −70°C). (Note that the term dry in this work, unless otherwise stated, signifies lyophilized from methanol.) The

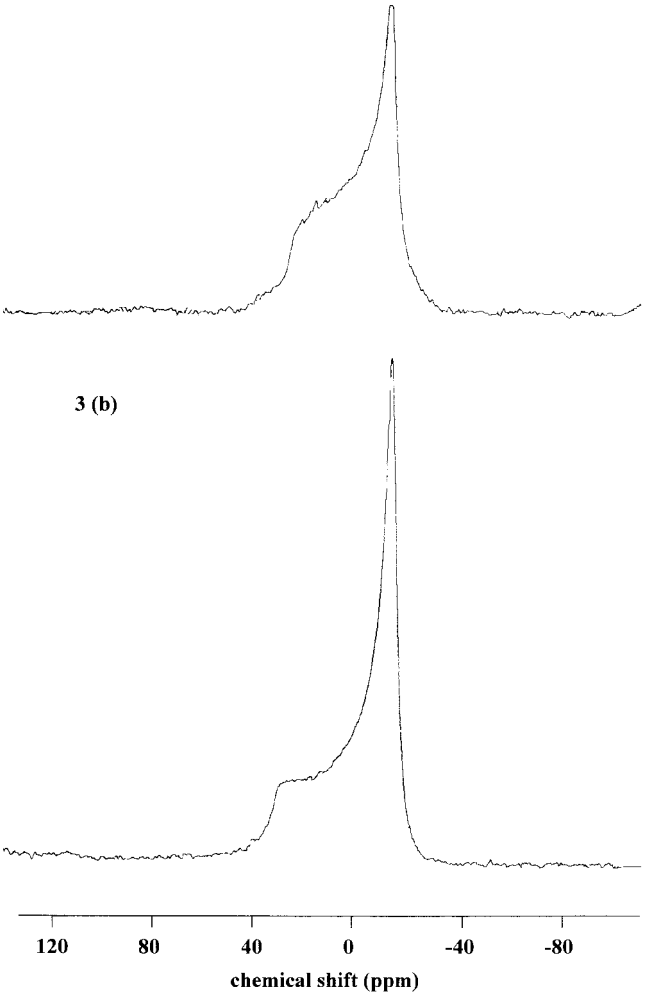

FIGURE 3 (*A*) Static ^{31}P NMR spectra of lyophilized powder of DTPC containing [1-^{13}C]Leu13-[2-^{13}C]Ala15 melittin; (*B*) DTPC containing [1-^{13}C]Leu13-[2-^{13}C]Ala15 melittin and hydrated with 50% w/v water at 30°C. Spectral parameters were as stated in Materials and Methods and 4096 scans.

adoption of gel phase in the latter case eliminates fast axial rotation of the peptide, which would project the dipolar interaction along the axis of reorientation and, depending upon orientation of the internuclear vector, scale the coupling measured (Langlais et al., 1999). Increased efficiency for cross-polarization between protons and carbon is an additional advantage gained by the reduction in molecular motion (Langlais et al., 1999). The RR distances observed for melittin in dry and hydrated lipid in the gel phase were the same and are listed together in Table 1. There were, however, several differences in distances measured by RR of melittin in DTPC compared with those of melittin as a powder lyophilized from methanol or water.

The distances determined by RR for [1-^{13}C]Leu13-[2-^{13}C]Ala15 melittin as a dry powder from methanol (4.0 Å) or in DTPC (3.8 Å) were the same within experimental uncertainty (±0.2 Å in lipid). The same level of agreement

was exhibited by [2-^{13}C]Leu13-[1-^{13}C]Ala15 melittin dried from methanol (5.2 Å) or in DTPC (5.0 Å). An appreciable difference between the dry powder and peptide in DTPC was seen in the distance between [1-^{13}C]Leu13 and [2-^{13}C]Leu16, which was 4.3 Å and 4.8 Å, respectively. The implication is that there is a conformational change in the proline region of melittin due to lipid binding.

A major difference in conformation of bound peptide with respect to the x-ray crystal structure near Pro14 is also implied from comparison of interatomic distances. Most noticeably, the distance measured by RR of [1-^{13}C]Leu13-[2-^{13}C]Ala15 melittin in lipid was 3.8 Å, which is to be compared with 4.5 Å in the x-ray structure. Although the differences seen for [2-^{13}C]Leu13-[1-^{13}C]Ala15 and [1-^{13}C]Leu13-[2-^{13}C]Leu16 are not so large, they are at the limit of experimental uncertainty or greater. The RR versus x-ray distances were 5.0 versus 5.5 Å and 4.8 versus 4.5 Å, respectively. By contrast, only one of the three interatomic distances measured in this region by RR of peptide bound to DTPC could be considered to be outside the bounds of experimental uncertainty from the values derived from the atomic coordinates of melittin bound to DPC micelles. The least agreement is for [1-^{13}C]Leu13-[2-^{13}C]Leu16, where 4.8 Å and 4.3 Å are the respective RR and solution NMR-derived distances. The corresponding distances for [1-^{13}C]Leu13-[2-^{13}C]Ala15 are 3.8 versus 4.1 Å, and for [2-^{13}C]Leu13-[1-^{13}C]Ala15 are 5.0 versus 5.1 Å.

Molecular modeling was undertaken to interpret the RR distances in terms of the x-ray and micellar structures, and the proposed transmembrane structure of Smith et al. (1994). Modeling also allowed investigation of possible structural changes that could be observed between melittin in dry and hydrated membranes. However, the distances measured for melittin in dry and hydrated gel-phase membranes were the same by RR. Fig. 4 shows the model structures generated by DYANA using the x-ray structure of melittin but incorporating constraints derived from the RR data. To provide a point of reference, they are superimposed upon the x-ray structure such that the N-terminal helices overlay with both stick (Fig. 4 *A*) and ribbon (Fig. 4 *B*) representations shown. Similar structures were calculated when using the RR distances obtained from melittin lyophilized from methanol. For purposes of comparison, model structures were also calculated including the RR constraints with constraints derived from the solution NMR structure of melittin in DPC micelles. The more hydrophobic environment of the micelle is closer to that of the lipid used for RR than the aqueous environment from which the x-ray crystal was produced. Calculations using constraints from either the x-ray or DPC structures, however, gave the same final model structures. Virtually the same structures for melittin were generated using SYBYL 6.5, an alternative modeling package.

Table 2 lists the interhelical angles determined for melittin on the basis of our RR data and other work. They

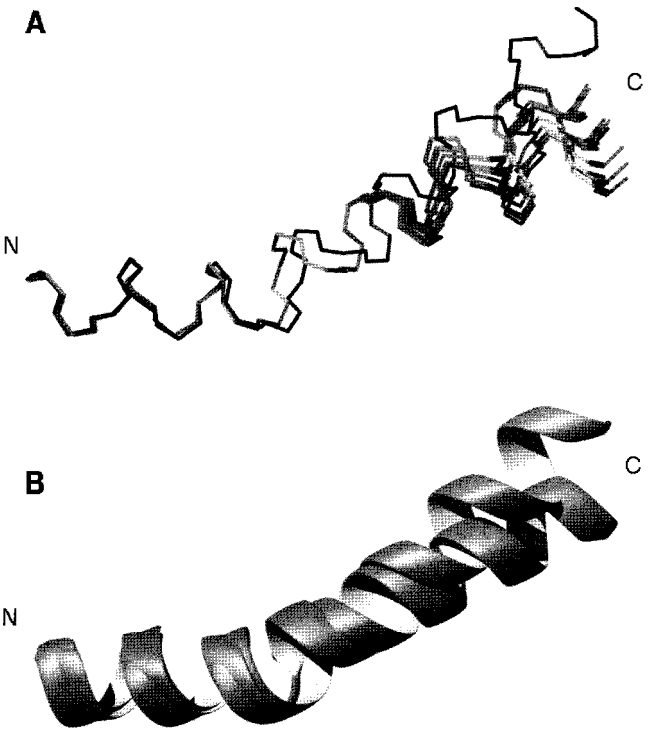

FIGURE 4 Comparison of model structures of melittin determined by x-ray crystallography (Terwilliger and Eisenberg, 1982) and by incorporation of distance constraints derived from RR measurements of peptide in DTPC: (*A*) Backbone representations of the x-ray structure (*black*) and the family of 20 model structures determined by simulated annealing incorporating constraints from the RR experiments (*gray*); (*B*) Cartoon representation of the x-ray and mean RR-derived model structures, clearly showing the difference in interhelical angle. For comparison, the structures are superimposed over residues 1–10. The figure was produced using MOLMOL (Koradi et al., 1996).

were measured at the intersection of the two lines drawn through the axes of the helices defined by residues 1–13 and 17–26. A common definition is crucial for comparison because the angle is sensitive to the number of residues employed. It should be noted that earlier studies (Terwilliger and Eisenberg, 1982; Inagaki et al., 1989; Bazzo et al., 1988; Okada et al., 1994) used different

TABLE 2 Interhelical angles (residues 1–13 and 17–26) for the structures of melittin in different environments

Structure of melittin	Interhelical angles
Powder, lyophilized from methanol	130°±9°
DTPC, dry or hydrated gel phase	142°±3°
Crystal (Terwilliger and Eisenberg, 1982)	129°*
DPC micelles (Inagaki *et al.*, 1989)	126°±15°†

*Note that this angle comes to 126° with MOLMOL when residues 5–9 and 14–20 are used to define the interhelical angles, rather than the 120° reported earlier (Terwilliger and Eisenberg, 1982; Dempsey, 1990).
†The authors (Inagaki *et al.*, 1989) quote the angle as 135°±15° using residues 1–10 and 13–26 to define the α-helical segments. The ±15° range stated here is their estimate.

numbers of residues to define the α-helical segments. The angles measured between the N- and C- terminal α-helices in the structures modeled for melittin bound to DTPC (Fig. 4 *A*) came to 142° ± 3° (where the distribution in angle represents the range in angles for the generated structures), larger than the angle of 129° obtained from the crystal structure (Terwilliger and Eisenberg, 1982). In DPC micelles (Inagaki et al., 1989), this angle came to 126° ± 15°, similar to that obtained using the RR constraints for melittin lyophilized from methanol, 130° ± 9°. Despite variation in internuclear spacing (Table 1), it appears that the interhelical angle is relatively insensitive to environment. Exceptions to this trend do exist in the literature. Approximately 160° was reported for melittin dissolved in methanol (Bazzo et al., 1988; Dempsey, 1990), whereas an angle of 86° ± 34° was reported on the basis of transferred NOE for melittin bound to PC vesicles (Okada et al., 1994). Experimental differences may be responsible. Low peptide concentration (7×10^{-4} mmol/μL and 50:1 peptide/lipid) and high hydration apply to the latter study, for example, which may result in a surface rather than the transbilayer arrangement as reported in aligned multilayers (Smith et al., 1994).

In our earlier study, 10 analogs of melittin labeled with ^{13}C at the peptide carbonyl were incorporated into DTPC membranes aligned between glass plates (Smith et al., 1994). Reduced CSA consistent with a transmembrane arrangement in which N- and C-terminal helices possess a similar orientation close to the bilayer normal were recorded in the liquid-crystalline phase. The bend angle was suggested to be the same as for melittin in methanol (~160°) (Bazzo et al., 1988). Although the interhelical angle (139°–145°) measured here for melittin in gel-phase DTPC is greater than in crystals of the peptide, it is less than that indicated in aligned multilayers and implies a significant difference in conformation around the proline residue. One possible explanation for the smaller value may be that DTPC was in the gel phase, whereas the aligned bilayer was in the fluid phase. Hydration and lipid phase can affect the conformation and location of membrane peptides (Hirsh et al., 1996), and this may be reflected in local changes in secondary structure of melittin as observed by RR. The distinction between phases is particularly marked in DTPC that interdigitates in the gel state. Interdigitation reduces the bilayer repeat distance by ~20 Å (Kim et al., 1987a,b). These considerations exemplify the limitations of RR (Langlais et al., 1999) for structure determination of membrane peptides. RR experiments require studies of dry powders or at low temperature, and distance measurements are restricted to a particular section of the molecule. In the present study, we focused on the proline region of melittin in DTPC either as a dry powder or as a hydrated gel phase, and this may explain why the angle between the α-helices may be less than in fluid-phase bilayers. Intriguingly, however, a recent solid-state NMR study of ^{13}C-labeled analogs of melittin bound to magnetically aligned DMPC, the ester-linked version of DTPC, in the liquid crystalline state identified ~140° and ~160° as possible values for the interhelical angle (Naito et al., 2000).

Our data imply that melittin in a hydrophobic environment adopts a conformation with an interhelical angle that does not differ greatly from crystals prepared from aqueous solution. This observation applies to peptide lyophilized from methanol and to the structure previously reported for melittin bound to DPC micelles (Inagaki et al., 1989) but is less applicable to peptide bound to DTPC in hydrated gel state and dry form. However, given the range of experimental conditions, this is a remarkable finding. The multilamellar systems utilized for solid-state NMR, for instance, have much lower water content and curvature than the micelles of solution-state NMR work. There appears to be a tendency toward a bigger interhelical angle in planar membranes (Smith et al., 1994; Naito et al., 2000). Here we see an increase relative to crystalline melittin of ~10° in DTPC in gel-state multilamellar dispersion, whereas a similar or greater increase was concluded for aligned bilayers of DTPC (Smith et al., 1994) and DMPC (Naito et al., 2000) in the liquid-crystalline state.

CONCLUSIONS

The conformation of melittin in DTPC lipid was determined using rotational resonance NMR spectroscopy. A larger interhelical angle at Pro14 was observed in structures derived from RR data of melittin in dry and gel phase DTPC lipid (139°–145°) than in peptide crystallized from aqueous solution (129°) (Terwilliger and Eisenberg, 1982). The angle is not as great as deduced in our work for melittin in aligned fluid-phase DTPC membranes (160°) (Smith et al., 1994). This difference might reflect a distinction in peptide structure between ordered and disordered lipid environments and/or result from DTPC being interdigitated in the gel phase, which produces a thinner membrane. Our results, however, suggest that the interhelical angle in melittin is relatively insensitive to significant changes in environment, from largely hydrophobic membranes and powders lyophilized from methanol to crystals prepared from aqueous solution. This study demonstrates an application of RR techniques to the structural analysis of membrane peptides and could be applied to more complex systems, including membrane-bound receptors (Williamson et al., 2000) and ion channels. Currently, RR studies of a melittin-inhibitor complex are underway.

It is a pleasure to thank Dr. F. G. Prendergast for the generous synthesis of labeled melittin analogs. We also gratefully acknowledge Dr. C. Glaubitz

for his valuable help and advice with the RR simulations and initial experiments and Dr. Y. Lin for her help with the SYBYL modeling.
Financial support was received from the Australian Research Council and the National Science Foundation (INT-9316922).

REFERENCES

Bachar, M., and O. M. Becker. 2000. Protein-induced membrane disorder: a molecular dynamics study of melittin in a dipalmitoylphosphatidylcholine bilayer. *Biophys. J.* 78:1359–1375.

Barlow, D. J., and J. M. Thornton. 1988. Helix geometry in proteins. *J. Mol. Biol.* 201:601–619.

Bazzo, R., M. J. Tappin, A. Pastore, T. S. Harvey, J. A. Carver, and I. D. Campbell. 1988. The structure of melittin: a ^{1}H-NMR study in methanol. *Eur. J. Biochem.* 173:139–146.

Bello, J., H. R. Bello, and E. Granados. 1982. Conformation and aggregation of melittin: dependence on pH and concentration. *Biochemistry.* 21:461–465.

Bernëche, S., M. Nina, and B. Roux. 1998. Molecular dynamics simulation of melittin in a dimyristoylphosphatidylcholine bilayer membrane. *Biophys. J.* 75:1603–1618.

Bielecki, A., and D. P. Burum. 1995. Temperature dependence of ^{207}Pb MAS spectra of solid lead nitrate: an accurate, sensitive thermometer for variable-temperature MAS. *J. Magn. Reson. Ser. A.* 116:215–20.

Carpino, L. A., and G. Y. Han. 1972. The 9-fluorenylmethoxycarbonyl amino-protecting group. *J. Org. Chem.* 37:3404–3409.

Cross, T. A., and S. J. Opella. 1994. Solid-state NMR structural studies of peptides and proteins in membranes. *Curr. Opin. Struct. Biol.* 4:574–581.

Dawson, C. R., A. F. Drake, J. Heliwell, and R. C. Hider. 1978. The interaction of bee melittin with lipid bilayer membranes. *Biochim. Biophys. Acta.* 510:75–86.

Deisenhofer, J., and H. Michel. 1989. The photosynthetic reaction center from the purple bacterium *Rhodopseudomonas viridis*. *Science.* 245: 1463–1473.

Dempsey, C. E. 1990. The actions of melittin on membranes. *Biochim. Biophys. Acta.* 1031:143–161.

Drake, A. F., and R. C. Hider. 1979. The structure of melittin in lipid bilayer membranes. *Biochim. Biophys. Acta.* 555:371–373.

Dufourc, E. J., C. Mayer, J. Stochrer, G. Althoff, and G. Kothe. 1992. Dynamics of phosphate head groups in biomembranes: comprehensive analysis using phosphorus-31 nuclear magnetic resonance lineshape and relaxation time measurements. *Biophys. J.* 61:42–57.

Fields, C. G., G. B. Fields, R. L. Fields, and T. A. Cross. 1989. Solid phase peptide synthesis of ^{15}N-gramicidins A, B, and C and high performance liquid chromatographic purification. *Int. J. Peptide Protein Res.* 33: 298–303.

Güntert, P., C. Mumenthaler, and K. Wüthrich. 1997. Torsion angle dynamics for NMR structure calculation with the new program DYANA. *J. Mol. Biol.* 273:283–298.

Henderson, R., J. M. Baldwin, T. A. Ceka, F. Zemlic, E. Beckmann, and K. H. Downing. 1990. Model for the structure of bacteriorhodopsin based on high-resolution electron cryo-microscopy. *J. Mol. Biol.* 213: 899–929.

Hing, F. S., P. R. Maulik, and G. G. Shipley. 1991. Structure and interactions of ether- and ester-linked phosphatidylethanolamines. *Biochemistry.* 30:9007–9015.

Hirsh, D. J., J. Hammer, W. L. Maloy, J. Blazyk, and J. Schaefer. 1996. Secondary structure and location of a magainin analogue in synthetic phospholipid bilayers. *Biochemistry.* 35:12733–12741.

Hristova, K., C. E. Dempsey, and S. H. White. 2001. Structure, location, and lipid perturbations of melittin at the membrane interface. *Biophys. J.* 80:801–811.

Inagaki, F., K. Shimada, K. Kawaguchi, M. Hirano, I. Terasawa, T. Ikura, and N. Go. 1989. Structure of melittin bound to perdeuterated dodecylphosphocholine micelles as studied by two-dimensional NMR and distance geometry calculations. *Biochemistry.* 28:5985–5991.

Kaiser, E., R. L. Colescott, C. D. Bossinger, and P. I. Cook. 1970. Color test for detection of free terminal amino groups in the solid-phase synthesis of peptides. *Anal. Biochem.* 34:595–598.

Kim, J. T., J. Mattai, and G. G. Shipley. 1987a. Gel phase polymorphism in ether-linked dihexadecylphosphatidylcholine bilayers. *Biochemistry.* 26:6592–6598.

Kim, J. T., J. Mattai, and G. G. Shipley. 1987b. Bilayer interactions of ether- and ester-linked phospholipids: dihexadecyl- and dipalmitoylphosphatidylcholines. *Biochemistry.* 26:6599–6603.

Knoppel, E., D. Eisenberg, and W. Wickner. 1979. Interactions of melittin, a preprotein model, with detergents. *Biochemistry.* 28:4177–4181.

Koradi, R., M. Billeter, and K. Wüthrich. 1996. MOLMOL: a program for display and analysis of macromolecular structures. *J. Mol. Graphics.* 14:51–55.

Laggner, P., K. Lohner, R. Koynova, and B. Tenchov. 1991. The influence of low amounts of cholesterol on the interdigitated gel phase of hydrated dihexadecylphosphatidylcholine. *Chem. Phys. Lipids.* 60:153–161.

Langlais, D. B., R. S. Hodges, and J. H. Davis. 1999. ^{13}C-^{13}C rotational resonance in a transmembrane peptide: a comparison of the fluid and gel phases. *Phys. Rev. E.* 59:5945–5957.

Levitt, M. H., D. P. Raleigh, F. Creuzet, and R. G. Creuzet. 1992. Theory and simulations of homonuclear spin pair systems in rotating solids. *J. Chem. Phys.* 92:6347–6364.

Lin, J.-H., and A. Baumgaertner. 2000. Stability of a melittin pore in a lipid bilayer: a molecular dynamics study. *Biophys. J.* 78:1714–1724.

Naito, A., T. Nago, K. Norisad, T. Mizuno, S. Tuzi, and H. Saito. 2000. Conformation and dynamics of melittin bound to magnetically oriented lipid bilayers by solid-state ^{31}P and ^{13}C NMR spectroscopy. *Biophys. J.* 78:2405–2417.

Okada, A., K. Wakamatsu, T. Miyzawa, and T. Higashijima. 1994. Vesicle-bound conformation of melittin: transfered nuclear Overhauser enhancement analysis in the presence of perdeuterated phosphatidylcholine vesicles. *Biochemistry.* 33:9438–9446.

Otoda, K., S. Kimura, and Y. Imanishi. 1992. Orientation change of glycopeptide in lipid bilayer membrane induced by lectin binding. *Biochim. Biophys. Acta.* 1112:1–6.

Peersen, O. B., M. Groesbeek, S. Aimoto, and S. O. Smith. 1995. Analysis of rotational resonance magnetization exchange curves from crystalline peptides. *J. Am. Chem. Soc.* 117:7228–7237.

Peersen, O. B., and S. O. Smith. 1993. Solid-state NMR approaches for studying membrane protein structure. *Concept Magn. Reson.* 5:303–317.

Rivett, D. E., A. Kirkpatrick, D. R. Hewish, W. Reilly, and J. A. Werkmeister. 1996. Dimerization of truncated melittin analogues results in cytolytic peptides. *Biochem. J.* 316:525–529.

Seelig, J. 1978. ^{31}P nuclear magnetic resonance and the head group structure of phospholipids in membranes. *Biochim. Biophys. Acta.* 515: 105–140.

Segrest, J. P., H. DeLoof, J. G. Dohlman, C. G. Brouillette, and G. M. Anantharamaiah. 1990. Amphiphatic helix motifs: classes and properties. *Proteins.* 8:103–117.

Separovic, F., R. Smith, C. S. Yannoni, and B. A. Cornell. 1990. Molecular sequence effect on the ^{13}C carbonyl chemical shift shielding tensor. *J. Am. Chem. Soc.* 112:8324–8328.

Sessa, G., J. H. Freer, G. Colacicco, and G. Weissmann. 1969. Interaction of a lytic polypeptide, melittin, with lipid membrane systems. *J. Biol. Chem.* 244:3575–3582.

Smith, R., F. Separovic, T. J. Milne, A. Whittaker, F. M. Bennett, B. A. Cornell, and A. Makriyannis. 1994. Structure and orientation of the pore-forming peptide, melittin, in lipid bilayers. *J. Mol. Biol.* 241: 456–466.

Stewart, J., and J. Stewart. 1984. Solid Phase Peptide Synthesis. Pierce Chemical Co., Rockford, IL.

Talbot, J. C., J. Dufourcq, J. DeBony, J.-F. Faucon, and C. Lussan. 1979. Conformational change and self association of monomeric melittin. *FEBS Lett.* 102:191–193.

Terwilliger, T. C., and D. Eisenberg. 1982. The structure of melittin. II. Interpretation of the structure. *J. Biol. Chem.* 257:6016–6022.

Thompson, L. K., A. E. McDermott, J. Raap, C. M. van der Wielen, J. Lugtenburg, J. Herzfeld, and R. G. Griffin. 1992. Rotational resonance NMR study of the active site structure in bacteriorhodopsin: conformation of the Schiff base linkage. *Biochemistry.* 31: 7931–7938.

Tosteson, M. T., and D. C. Tosteson. 1981. The sting: melittin forms channels in lipid bilayers. *Biophys. J.* 36:109–116.

Vogel, H. 1981. Incorporation of melittin into phosphatidylcholine bilayers: study of binding and conformational changes. *FEBS Lett.* 134:37–42.

Vogel, H. 1987. Comparison of the conformation and orientation of alamethicin and melittin in lipid membranes. *Biochemistry.* 26:4562–4572.

Vogel, H., and F. Jähnig. 1986. The structure of melittin in membranes. *Biophys. J.* 50:573–582.

Warwicker, J., and H. C. Waston. 1982. Calculation of the electric potential in the active site left due to alpha-helix dipoles. *J. Mol. Biol.* 157: 617–679.

Williamson, P. T. F., B. Bonev, F. J. Barrantes, and A. Watts. 2000. Structural characterization of the M4 transmembrane domain of the acetylcholine receptor: an NMR study. *Biophys. J.* 44:117.